THE FASEB JOURNAL • RESEARCH • www.fasebj.org

PTENα regulates endocytosis and modulates olfactory function

Yuyao Yuan,*,† Xuyang Zhao,† Pan Wang,*,† Fan Mei,*,† Juntuo Zhou,* Yan Jin,* Michael A. McNutt,* and Yuxin Yin*,†,‡,1

*Institute of Systems Biomedicine, †Department of Pathology, School of Basic Medical Sciences, and ‡Peking–Tsinghua Center for Life Sciences, Peking University Health Science Center, Beijing, China

ABSTRACT: Phosphatase and tensin homolog deleted on chromosome 10 (PTEN) α is the first identified isoform of the well-known tumor suppressor PTEN. PTENα has an evolutionarily conserved 173-aa N terminus compared with canonical PTEN. Recently, PTENα has been shown to play roles in multiple biologic processes including learning and memory, cardiac homeostasis, and antiviral immunity. Here, we report that PTENα maintains mitral cells in olfactory bulb (OB), regulates endocytosis in OB neurons, and controls olfactory behaviors in mice. We show that PTENα directly dephosphorylates the endocytic protein amphiphysin and promotes its binding to adaptor-related protein complex 2 subunit β1 (Ap2b1). In addition, we identified mutations in the N terminus of PTENα in patients with Parkinson disease and Lewy-body dementia, which are neurodegenerative disorders with early olfactory loss. Overexpression of PTENα mutant H169N in mice OB reduces odor sensitivity. Our data demonstrate a role of PTENα in olfactory function and provide insight into the mechanism of olfactory dysfunction in neurologic disorders.—Yuan, Y., Zhao, X., Wang, P., Mei, F., Zhou, J., Jin, Y., McNutt, M. A., Yin, Y. PTENα regulates endocytosis and modulates olfactory function. FASEB J. 33, 11148–11162 (2019). www.fasebj.org

KEY WORDS: Ap2b1 · olfaction · neurodegenerative disease · amphiphysin

Olfaction is important in humans for the maintenance of quality of life and avoidance of danger. In rodents, essential activities such as feeding, mating, and maternal behavior are all based on olfaction. It is common for aged people to undergo olfactory deficits, particularly in many neurodegenerative diseases. In Parkinson disease (PD), Alzheimer disease (AD), and Lewy-body dementia (LBD), ~90% of patients show olfactory loss at early stages, which usually occurs years before typical symptoms such as motor deficits and cognition impairment are identified (1–3). Although various hypotheses have been put forth to account for olfactory loss in neurodegenerative diseases (1, 2, 4–7), the underlying pathogenesis remains to be explained.

The olfactory bulb (OB) relays odor signals from olfactory sensory neurons of the olfactory epithelium to central brain regions and processes odor information as well. The OB is a highly laminated structure made up of multiple layers. Mitral cells are the projection neurons of OB and are distributed in the mitral cell layer, projecting information from olfactory epithelium to higher central cortices. The most central region of OB is the granule cell layer, where newborn neurons are continuously generated after birth to integrate into OB neural circuits. Mitral cells form synapses with olfactory sensory neuron terminals in the glomerular layer of OB and granule cells in the granule cell layer, which involves mitral cells in complicated neuron circuits (8, 9).

In the brain, endocytosis is an important process that regulates membrane receptor trafficking and recycling and neuritogenesis and axon guidance during neural development (10–12). Amphiphysin I is a well-characterized protein that plays a central role in regulation of endocytosis (13). This protein is a phosphoprotein expressed predominantly in the brain, and it belongs to the Bin-amphiphysin-Rvs (BAR) domain protein family, which is a group of proteins capable of sensing membrane curvature and mediating endocytosis (13). Amphiphysin is involved in the pathogenesis of certain types of

ABBREVIATIONS: AAV, adeno-associated virus; AD, Alzheimer disease; Ap2b1, adaptor related protein complex 2 subunit β1; BAR, Bin-amphiphysin-Rvs; BIN1, bridging integrator 1; BrdU, 5-bromo-2′-deoxyuridine; CCP, clathrin-coated pit; CME, clathrin-mediated endocytosis; co-IP, co-immunoprecipitation; DIV, days *in vitro*; EGF, epidermal growth factor; EGFR, epidermal growth factor receptor; GFP, green fluorescent protein; GO, gene ontology; HA, human influenza hemagglutinin; HEK, human embryonic kidney; His, polyhistidine; IP, immunoprecipitation; LBD, Lewy-body dementia; NR2B, glutamate receptor ionotropic, NMDA 2B; OB, olfactory bulb; PD, Parkinson disease; PGP9.5, ubiquitin C-terminal hydrolase L1; PTEN, phosphatase and tensin homolog deleted on chromosome 10; SVZ, subventricular zone; TH, tyrosine hydroxylase

[1] Correspondence: Institute of Systems Biomedicine, School of Basic Medical Sciences, Peking University Health Science Center, 38 Xueyuan Rd., Haidian District, Beijing 100191, P.R. China. E-mail: yinyuxin@hsc.pku.edu.cn

doi: 10.1096/fj.201900588RR
This article includes supplemental data. Please visit *http://www.fasebj.org* to obtain this information.

0892-6638/19/0033-11148 © FASEB

neurodegenerative disorders (14, 15). Genomic alteration of amphetamine (*AMPH*), which encodes amphiphysin, is identified in many developmental deficits in humans (16–18), and a mouse model with amphiphysin knockout demonstrated decreased synaptic vesicle recycling efficiency and cognitive deficits (19).

Phosphatase and tensin homolog deleted on chromosome 10 (PTEN)α was previously identified as an isoform of PTEN. PTENα translates from the 5′UTR region of the same mRNA as PTEN, containing an evolutionarily conserved 173-aa N-terminal extension (20, 21). Recently, PTENα is shown to play important roles in maintenance of mitochondrial structure and energy metabolism (21), modulation of hippocampal long-term potentiation and processes of learning and memory (22), regulation of cardiac homeostasis and mitophagy (23, 24), and promotion of type I IFN responses and antiviral immunity (25). However, it likely has other biologic functions that have not been characterized. Our preliminary data showed that PTENα is expressed predominantly in the OB of the mouse brain. In view of the fact that PTENα plays important roles in modulation of neural activity (22), we sought to determine whether PTENα and olfactory function are linked.

In this study, we show that PTENα is involved in regulation of olfactory function and regulation of endocytosis in the mouse OB. Moreover, we identify PTENα mutations in human neurodegenerative diseases with early olfactory loss. Our data show that these mutations are dominant negative and possibly contribute to the pathogenesis of olfactory dysfunction.

MATERIALS AND METHODS

Mice

The PTENα-specific knockout mouse model ($Pten\alpha^{mu/mu}$ mice) used in this study is generated as previously described (22). Briefly, mouse embryonic stem cells were electroporated with a knockin-targeting construct designed to replace 347CTG and 362CTG of the PTEN gene with GGA. All procedures followed the Peking University *Guidelines for Using Animals in Intramural Research* and were approved by the Animal Care and Use Committee of Peking University. All efforts were made to minimize animal suffering. C57BL/6 mice were housed in a climate-controlled facility (22 ± 2°C) and maintained under standard conditions on a 14/10-h light/dark cycle, with water and food *ad libitum*. For all tests, littermates of the same sex were randomly assigned to experimental groups. For behavioral tests, only male mice of indicated age were used, and the mice were housed individually for at least 2 wk before experiment.

Cell lines

Human embryonic kidney (HEK) 293T cells used in this study were from the American Type Culture Collection (Manassas, VA, USA). HEK293T cells are originally derived from a human female fetal kidney. The cells were maintained in DMEM (Corning, Corning, NY, USA) supplemented with 10% fetal bovine serum (Hyclone Laboratories, Logan, UT, USA) in a 37°C incubator with 5% (v/v) CO_2. The insect cell line Sf9 was obtained from Thermo Fisher Scientific (Waltham, MA, USA) and cultured in Grace's insect medium (Thermo Fisher Scientific).

Antibodies

The following antibodies were used: mouse monoclonal anti-glial fibrillary acidic protein (Gfap) (1:50, 3670, RRID:AB_561049; Cell Signaling Technology, Danvers, MA, USA), rabbit monoclonal anti-Ki67 (1:200, RM-9106-S0, RRID:AB_2341197; Thermo Fisher Scientific), rabbit polyclonal anti-ubiquitin C-terminal hydrolase L1 (PGP9.5) (1:50, A014, RRID:AB_2756452; ABclonal, Woburn, MA, USA), rabbit polyclonal anti-amphiphysin I (1:1000, 13379-1-AP, RRID:AB_2226789; Proteintech, Rosemont, IL, USA), mouse monoclonal anti-NR2B (1:1000, 610416, RRID:AB_397796; BD Biosciences, San Jose, CA, USA), mouse monoclonal anti–5-bromo-2′-deoxyuridine (BrdU) (clone B44) (1:15, 347580, RRID:AB_400326; BD Biosciences), rabbit polyclonal anti–*N*-cadherin (1:1000, sc-7939, RRID:AB_647794; Santa Cruz Biotechnology, Dallas, TX, USA), rabbit monoclonal anti-PTEN (1:1000, 9559, RRID:AB_390810; Cell Signaling Technology), rabbit polyclonal anti-phosphoserine (1:1000, ab9332, RRID:AB_307184; Abcam, Cambridge, MA, USA), rabbit polyclonal anti-tyrosine hydroxylase (TH) (1:50, RLT4638, RRID:AB_2756454; Ruiying, Heze, China), rabbit polyclonal anti-bridging integrator 1 (BIN1) (1:1000, RLT5352, RRID:AB_2756453; Ruiying), rabbit polyclonal anti-epidermal growth factor receptor (EGFR) (1:1000, YT1488, RRID:AB_2756456; ImmunoWay Biotechnology, Plano, TX, USA), mouse monoclonal anti-FLAG (1:5000, F3165, RRID:AB_259529; MilliporeSigma, Burlington, MA, USA), mouse monoclonal anti-human influenza hemagglutinin (HA) (1:5000, H3663, RRID:AB_262051; MilliporeSigma), mouse monoclonal anti-green fluorescent protein (GFP) (1:5000, RM1008, RRID:AB_2756458; RayAntibody, Beijing, China), mouse monoclonal anti-glyceraldehyde 3-phosphate dehydrogenase (GAPDH; 1:5000, RM2002, RRID:AB_2756459; RayAntibody), and rabbit monoclonal anti–β-actin (1:5000, PM053, RRID:AB_10598196; MBL International, Woburn, MA, USA).

Buried food pellet test

Male mice of appropriate age as previously described were chosen for this experiment. The mice were fed a food-restricted diet for 3 d, and the mice weighed about 20% less than the original weight on the first day. Each mouse was adapted for 3 min on 2 consecutive days. On the experimental day, a 0.5-g food pellet was buried ~1.5 cm below the surface of a 3-cm-thick layer of mouse bedding material. Any animal that did not find the food pellet within 3 min was removed and put back into its home cage. The restricted diet was continued, and the experiment was repeated the next day following the same procedure except that the buried food was in a different location. Latency for discovery of the food pellet was defined as the time interval between when the mouse was placed in the cage and when the mouse uncovered the food pellet and grasped it in its forepaws or teeth.

Olfactory sensitivity test

Male mice of appropriate age as previously described were chosen for this experiment. The mice were simultaneously presented with 2 cotton tips, 1 soaked with vehicle as a control and the other soaked with a specific odorant, ethyl vanillin. The 2 cotton tips were randomly switched between trials to avoid spatial learning. One trial was performed presenting 1 odorant concentration per day with increasing concentrations. Each trial lasted 3 min, and total number of investigations was recorded during the entire 3-min session for statistical analysis.

Odor habituation and dishabituation test

Male mice of appropriate age as previously described were chosen for this experiment. When a mouse is subjected to

repeated presentation of the same odor, the frequency of exploration should show progressive decrease. Then, the mouse is subjected to a novel odor, and the frequency of exploration should show instant increase.

The mice were subjected to a variety of different odors through cotton tips. The odorous stimulus was presented to the subjects for 2 min in 3 consecutive trials, with an intertrial interval of 1 min. The number of investigations of the subjects was recorded. A qualifying positive investigation was defined as a mouse in contact or 1–2 mm from the cotton tip. Odors are used in the following sequence: distilled water, ethyl vanillin, male mouse urine (diluted 1:50 in water) of stranger 1, male mouse urine (diluted 1:50 in water) of stranger 2, and female urine (diluted 1:50 in water).

PD98059 administration in mice

PD98059 was dissolved in 25% polyethylene glycol, 10% DMSO, and 0.9% saline to a final concentration of 2 mg/ml. PD98059 was administered intraperitoneally (10 mg/kg) 3 h before immunoprecipitation (IP) tests or behavioral tests were conducted.

BrdU staining

BrdU was administered intraperitoneally to mice for newborn neuron labeling. BrdU (50 mg/kg, i.p.) was administered daily for 12 consecutive days, and mice were euthanized for frozen sectioning. Sections were incubated in 2 M HCl at 37°C for 30 min and washed in PBS before immunostaining with BrdU antibody (BD Biosciences).

Immunofluorescence

All animals were deeply anesthetized and perfused through the heart. The brains were dissected out and postfixed in 4% paraformaldehyde at 4°C overnight and immersed in 20 and 30% sucrose each for 24 h at 4°C before embedding in optimal cutting temperature (OCT) compound and rapid freezing. Sections were cut using a cryostat (CM1850; Leica, Wetzlar, Germany) at a thickness of 15 μm and mounted on slides for the following experiments. On the day of immunofluorescence, the slices were first rinsed using PBS with 0.3% Triton X-100, blocked with 5% normal goat serum in PBS (blocking buffer) at room temperature for 60 min, and incubated with primary antibodies diluted in blocking buffer overnight at 4°C. Sections were washed with PBS and then incubated with secondary antibodies and DAPI for nuclei at room temperature. Sections were then washed and mounted with coverslips. Fluorescent signals were imaged with a confocal microscope (A1; Nikon, Tokyo, Japan). Positive cells were counted manually, and length and area on sections were analyzed by ImageJ software (National Institutes of Health, Bethesda, MD, USA).

Quantitative proteomic analysis

Mouse OB tissue was homogenized in RIPA buffer (50 mM Tris-HCl pH = 7.5, 150 mM NaCl, 1% Nonidet P-40, 0.1% SDS, protease inhibitor cocktail) for total protein sample preparation. In total, 100 μg of protein sample from each subject was loaded for SDS-PAGE and subjected to in-gel digestion for mass spectrometry analysis. The membrane fraction of mouse OB was isolated following the manufacturer's protocol for subcellular fractionation with a commercial kit (P1201; Applygen, Beijing, China). Protein samples of the membrane fraction (50 μg) from each group were processed according to the manufacturer's protocol for filter-aided sample preparation, followed by mass spectrometry analysis.

Peptides were separated by online reversed-phase nanoscale capillary liquid chromatography (Easy-nLC 1000; Thermo Fisher Scientific). The data-dependent mass spectra were acquired with the Linear Trap Quadropole Orbitrap Elite mass spectrometer (Thermo Fisher Scientific) equipped with a nanoelectrospray ion source (Thermo Fisher Scientific). Raw files were searched by Proteome Discoverer (v.1.4.1.14; Thermo Fisher Scientific) against the UniProt Human database (*https://www.uniprot.org/taxonomy/9606*). Search parameters were set as follows: enzyme with trypsin, up to 2 missed cleavages, carbamidomethyl cysteine as fixed modification, methionine oxidation as variable modifications. The false discovery rates were set at 0.01. The Database for Annotation, Visualization, and Integrated Discovery (DAVID; *http://david.abcc.ncifcrf.gov/*) was used to retrieve the Gene Ontology Consortium (GOC, *http://geneontology.org/*) and Kyoto Encyclopedia of Genes and Genomes (KEGG; *https://www.genome.jp/kegg/kegg1.html*) annotations for enrichment analysis of the differentially expressed proteins.

Pull-down assays

Pull-down assays were conducted as previously described (22). Briefly, exogenous proteins were expressed in HEK293T cells, pulled down by *S*-tag agarose or FLAG agarose, and incubated with mouse OB tissue lysate at 4°C for 3 h. The proteins were then eluted from agarose with glycine-HCl buffer (pH = 3.5), neutralized with Tris-HCl buffer (pH = 8.0), and subjected to mass spectrometry. Parameters of MS and enrichment analysis methods are the same as described in proteomic analysis. Interaction networks of proteins are analyzed in STRING (*https://string-db.org/*).

Quantitative Western blot and o-immunoprecipitation

Cells were extracted and lysed in lysis buffer (50 mM Tris-pH 7.5, 150 mM NaCl, 0.5% Triton X-100) freshly supplemented with 1 mM PMSF and protease inhibitor. Protein concentrations were measured by bicinchoninic acid assay (Thermo Fisher Scientific), and an equal amount of protein was loaded in each lane for SDS-PAGE. For quantification analysis, the blots were analyzed using ImageJ software.

For IP experiments, cell lysate was incubated with antibody against GFP tag or FLAG tag at 4°C for 2 h, followed by incubation with protein A/G agarose at 4°C for 1 h. The protein-agarose complex mixture was washed in washing buffer containing 0.1% Nonidet P-40 and subjected to Western blot to evaluate protein interaction.

Primary culture of OB neurons

Mouse pups of postnatal d 1 were used for OB neuron cultures. Pups were decapitated, and heads were dissected in 10-mm dishes with HBSS. OBs were carefully removed and incubated in 0.25% trypsin in a 37°C water bath for 30 min for dissociation. The cells were gently triturated, centrifuged, and counted after trypsin inactivation by fetal bovine serum. In total, 2.0×10^4 cells were plated in each well of 96-well plates for quantification of FITC-transferrin uptake, and 1.0×10^5 cells were plated in glass bottom 35-mm dishes for confocal imaging.

FITC-transferrin uptake assay

OB neurons cultured at 10 d *in vitro* (DIV)10 were incubated in 0.05 mg/ml FITC-transferrin (Jackson Immunoresearch Laboratories, West Grove, PA, USA) for 5 or 10 min in neurobasal

medium without B27 and Glutamax (Thermo Fisher Scientific). Neurons cultured in 96-well plates were lysed in 30 μl of lysis buffer (50 mM Tris-HCl pH 7.4, 150 mM NaCl, 0.5% Triton X-100 with protease inhibitor cocktail), and internalized fluorescent intensity and protein concentration was determined using a microplate reader (Flexstation 3; Molecular Devices, Sunnyvale, CA, USA). Wells with protein quantity lower than 3 μg or higher than 10 μg were eliminated from statistical analysis.

In vitro phosphatase assay

FLAG-amphiphysin was expressed in HEK293T cells and purified with FLAG agarose. Polyhistidine (His)-tagged amphiphysin and His-tagged PTENα were expressed in Sf9 cells and purified using Ni-nitrilotriacetic acid agarose. For the phosphatase assay, purified FLAG-amphiphysin or His-amphiphysin was incubated with purified His-PTENα or not in dephosphorylation buffer (20 mM HEPES, 1 mM $MgCl_2$, 1 mM EDTA, 1 mM DTT, and 0.1 mg/ml bovine serum albumin) for 1 h at 37°C. The resultant protein mixture was subjected to label-free mass spectrometry quantification of phosphorylated peptides for further analysis of potential target sites on amphiphysin.

Human genome sequencing of blood specimens

Human blood specimens from 40 normal human controls and 40 patients with neurodegenerative diseases were collected from local hospitals. For sequencing analysis, genomic DNA was extracted from blood samples using the Tianamp Blood DNA Kit (Tiangen, Beijing, China) and then used as templates for PCR amplification. Primers for PTENα exon1 sequencing are: forward, 5′-GCTTCTCCTGAAAGGGAAGGT-3′; reverse, 5′-ACTCCCACGTTCT-AAGAGAGT-3′. Allele frequencies in general population are refered to Genome Aggregation Database (gnomAD, *http://gnomad.broadinstitute.org/*).

Quantification and statistical analysis

Quantification results are shown as means ± SEM. Values of $P < 0.05$ (2-tailed Student's t test) were considered significant and were provided by Prism (GraphPad, La Jolla, CA, USA).

RESULTS

PTENα is highly expressed in the mouse OB, and levels of its expression vary temporally

Preliminary data from our laboratory showed that PTENα is expressed in different regions of the brain in mice (22). However, distribution of PTENα expression varies over these different brain regions. PTENα is expressed in the OB at a level that is obviously higher than other brain regions (**Fig. 1*A***; lane 1 *vs.* 2–8), which strongly suggests that PTENα plays an important role in the OB.

A large proportion of neurons in the OB are generated after birth and are renewed continuously throughout life. Therefore, a number of genes in the OB are expressed at different levels over different stages of development. We were thus led to consider whether PTENα expression in the OB varies with age. By evaluating PTENα protein levels in the mouse OB at different ages, we found PTENα expression levels in the OB gradually increase prior to adulthood (Fig. 1*B*; lanes 1–2) and decline with increasing age (Fig. 1*B*; lanes 3–4). Adult neurogenesis takes place with a similar spatial and temporal pattern (26), indicating PTENα may be involved in this process. This evidence suggests that PTENα plays an important role in the OB of adult mice.

PTENα-deficient mice exhibit impaired olfactory function and decrease in mitral cell number of OB

As previously described, we generated a mouse model with PTENα-specific ablation by editing the translation initiation codon of PTENα (22). These mice are designated $Pten\alpha^{\mu/\mu}$, and their wild-type littermates are designated $Pten\alpha^{+/+}$ in the text that follows. Evaluation of protein levels in OB tissue showed PTENα expression is ablated, whereas PTEN levels were not influenced (Supplemental Fig. S1*A*). We then sought to determine whether PTENα depletion influences olfactory function *in vivo* by

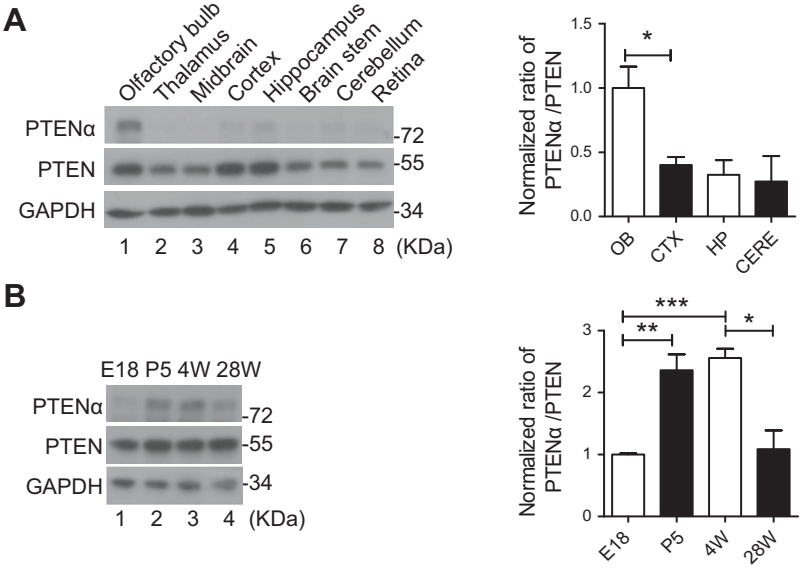

Figure 1. Expression level of PTENα is high in the mouse OB and shows temporal variation. *A*) Western blotting showing PTENα protein levels in different regions of the brain using 3-mo-old wild-type mice. Ratios of PTENα:PTEN in OB, cortex (CTX), hippocampus (HP), and cerebellum (CERE) from 3 independent experiments were statistically analyzed; $P = 0.0281$. *B*) PTENα levels were evaluated at different developmental stages. OBs from embryonic wild-type mice of d 18 (E18) and postnatal mice on d 5 (P5) and 1 and 7 mo were dissected for Western blot as shown in the figure. Ratios of PTENα:PTEN from 3 independent experiments were statistically analyzed ($P = 0.0063$, 0.0005, and 0.0121 left to right, respectively). GAPDH, glyceraldehyde 3-phosphate dehydrogenase. $^*P < 0.05$, $^{**}P < 0.01$, $^{***}P < 0.001$.

conducting a behavioral test called the buried food pellet test to assess general olfactory function in mice. The food-finding latency was significantly extended in *Ptenα*$^{\mu/\mu}$ mice as compared with *Ptenα*$^{+/+}$ mice (**Fig. 2*A***). To further evaluate the function of PTENα in olfactory processes, we compared olfactory sensitivity in mice of both genotypes. In comparing the frequency of exploration of a series of concentrations of odors, *Ptenα*$^{\mu/\mu}$ mice showed reduced odor sensitivity compared with *Ptenα*$^{+/+}$ littermates (Fig. 2*B*). Another behavioral assay, called odor habituation-dishabituation, was conducted to evaluate the ability to discriminate different odors. However, no significant difference in the 2 genotypes was found in this test, indicating normal ability to discriminate different odors in PTENα-deficient mice (Fig. 2*C*).

To better understand the pathogenesis underlying olfactory deficits of *Ptenα*$^{\mu/\mu}$ mice, we evaluated the OB grossly and in microscopic sections for morphologic alterations. There was no grossly identifiable difference in direct observation of postfixed tissue (Fig. 2*D*), although measurement and statistical analysis of the width of the OB showed slight differences (Supplemental Fig. S1*B*). Hematoxylin and eosin staining of sagittal sections, which gives a clear histologic view of different brain regions, also showed no significant difference (Fig. 2*E*). We assessed the number of mitral cells, the projection neurons in mice OB by immunostaining for PGP9.5 (mitral cell marker). The number of mitral cells markedly decreased in *Ptenα*$^{\mu/\mu}$ mice OB as compared with *Ptenα*$^{+/+}$ mice (Fig. 2*F–H*). Additional assessment of other cell types in the OB by immunostaining with the antibody TH (Supplemental Fig. S1*C*), which labels TH-positive short axon interneurons in the periglomerular layer of OB, and glial fibrillary acidic protein (Supplemental Fig. S1*D*), which is a marker for astrocytes, showed no significant difference *in Ptenα*$^{\mu/\mu}$ mice OB as compared with *Ptenα*$^{+/+}$ mice. Analysis of reactive oxygen species levels in the OB by dihydroethidium staining also showed no difference in these 2 groups of mice (Supplemental Fig. S1*E*). These data strongly suggest that mitral cell loss accounts for olfactory dysfunction in *Ptenα*$^{\mu/\mu}$ mice.

The largest neurogenic pool in the adult mice brain is the subventricular zone (SVZ), where newborn neurons migrate along the rostral migratory stream to reach the OB (27). In the OB of the adult brain, sensory input modulates survival and neural circuit integration of newborn neurons (28–30). Considering that PTENα-deficient mice demonstrated attenuated odorant sensory input, we wondered whether adult neurogenesis in the OB was affected when PTENα was deleted. By the means of BrdU incorporation and immunostaining with a BrdU antibody, we identified significantly fewer BrdU-positive cells in the OB of PTENα-deficient mice as compared with *Ptenα*$^{+/+}$ littermates but not in the SVZ, as expected (Fig. 2*I, J*). Consistent with results of BrdU labeling in the SVZ, immunostaining of sections across SVZ with an antibody of Ki67, which is a marker for proliferating cells, showed no difference in these 2 mouse genotypes (Supplemental Fig. S1*F*). These results indicate PTENα plays an indispensable role in the maintenance of normal olfactory function.

PTENα deletion alters protein levels in OB of mice in pathways of synaptic vesicle cycle and endocytosis

In order to further evaluate the mechanism underlying impaired olfactory function and mitral cell loss at the molecular level, *Ptenα*$^{+/+}$ and *Ptenα*$^{\mu/\mu}$ mice OB tissue lysate was subjected to mass spectrometry for proteomic analysis. Proteins of differential expression between *Ptenα*$^{+/+}$ and *Ptenα*$^{\mu/\mu}$ were identified (Supplemental Fig. S2*A, B*), and results were subjected to gene ontology (GO) analysis of the enriched KEGG pathway (**Fig. 3*A***). Among pathways with enrichment in differentially expressed proteins, pathways of synaptic vesicle cycling and endocytosis seem most likely to account for olfactory function. Levels of differentially expressed proteins identified in pathways of synaptic vesicle cycling and endocytosis through proteomic quantification are shown in Fig. 3*B, C*, respectively.

Both synaptic vesicle cycling and endocytic pathways are correlated with membrane proteins. For more precise analysis of membrane proteins in mice OB, we conducted proteomic analysis of the membrane fraction of the OB from *Ptenα*$^{+/+}$ and *Ptenα*$^{\mu/\mu}$ mice. Differentially expressed proteins were identified, and GO analysis of biologic processes was conducted. Proteins involved in transport and axon development show obvious alteration (Fig. 3*D*). Levels of proteins involved in the biologic process of transport quantified by proteomic analysis are shown in Fig. 3*E*. Moreover, levels of several surface proteins, such as neurotrophic receptor tyrosine kinase 2 (Trkb), EGFR, and glutamate receptors, which are regulated by endocytosis and known to influence neural migration and survival, consistently are increased in the membrane fraction of *Ptenα*$^{\mu/\mu}$ mice OB (Fig. 3*F*).

Neurotransmitters are closely related to synaptic vesicle cycling and endocytosis, and we therefore evaluated total levels of 4 types of neurotransmitters in mouse OB tissue by means of liquid chromatography–mass spectrometry analysis including glutamate acid, GABA, choline, and serotonin. It came as a surprise that *Ptenα*$^{\mu/\mu}$ mice showed significantly increased levels of glutamate and increased glutamate acid:GABA ratios in the OB tissue compared with *Ptenα*$^{+/+}$ mice (Supplemental Fig. S2*C, D*). These findings raised the possibility that neurotransmitter disruption in *Ptenα*$^{\mu/\mu}$ mice results from disturbance of synaptic vesicle cycling and endocytosis.

PTENα interacts with endocytic proteins and regulates endocytosis in OB neurons

To further understand the role PTENα plays in the OB at the molecular level, we conducted pull-down assays in mouse OB tissue. Exogenous Mock/PTEN/PTENα were overexpressed in HEK293T cells, pulled down by S-tag agarose, incubated with mouse OB tissue, and subjected to mass spectrometric analysis. PTENα pulled down a group of mutually interacting endocytic proteins (**Fig. 4*A, B***). These proteins included amphiphysin,

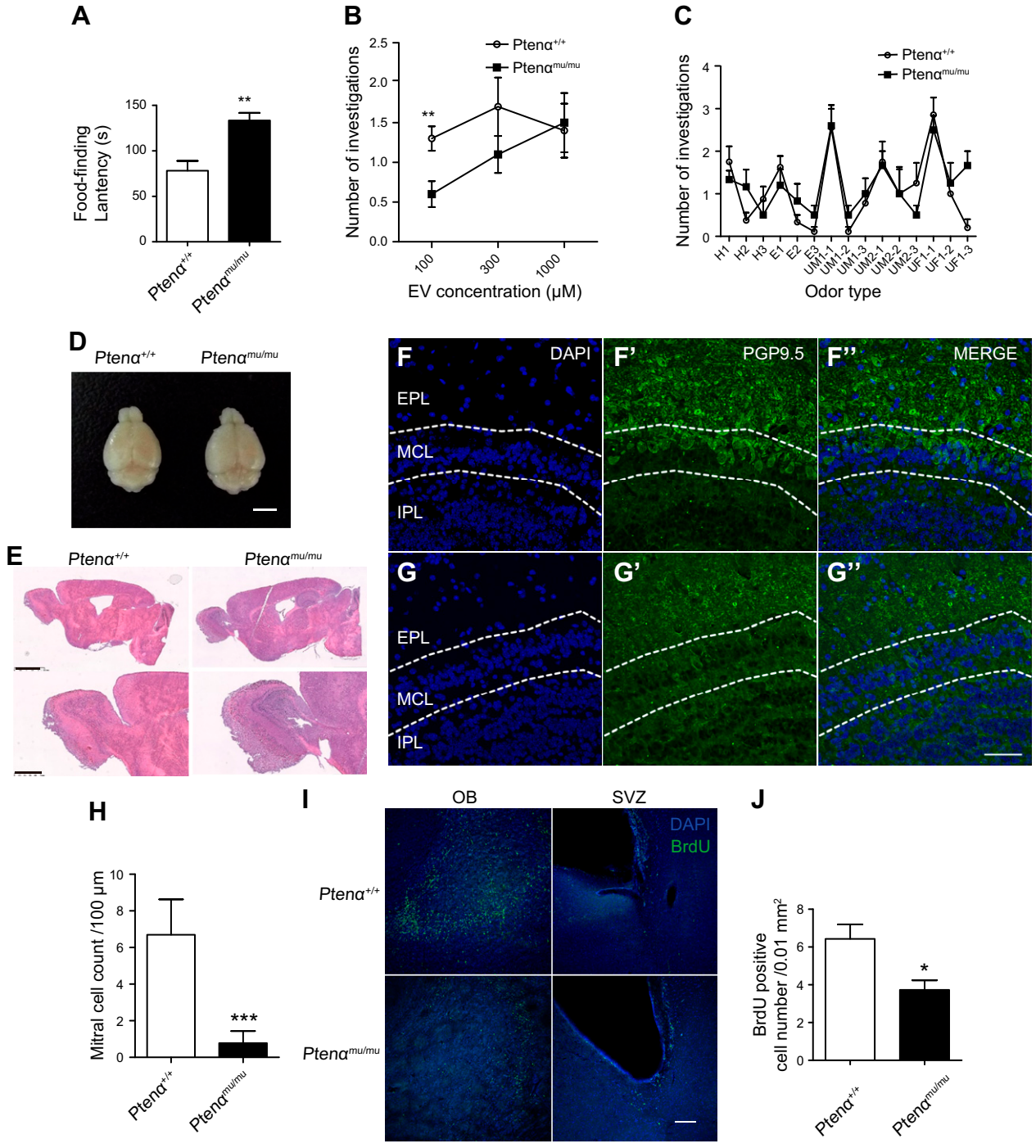

Figure 2. PTENα-deficient mice demonstrated impaired olfactory behavior and a significant decline in mitral cell number in OB. *A*) Buried food pellet tests with *Ptenα*$^{+/+}$ and *Ptenα*$^{\mu/\mu}$ 15-mo-old mice, n (*Ptenα*$^{+/+}$) = n (*Ptenα*$^{\mu/\mu}$) = 7. $P = 0.0017$. *B*) Olfactory sensitivity tests in *Ptenα*$^{+/+}$ and *Ptenα*$^{\mu/\mu}$ 4-mo-old mice, n (*Ptenα*$^{+/+}$) = n (*Ptenα*$^{\mu/\mu}$) = 10; $P = 0.0058$. *C*) Odor discrimination tests in *Ptenα*$^{+/+}$ and *Ptenα*$^{\mu/\mu}$ mice. Four-month-old mice, n (*Ptenα*$^{+/+}$) = n (*Ptenα*$^{\mu/\mu}$) = 10. Each odor was presented in 3-consecutive trials. H, distilled water; UF1, urine of female stranger 1UM1, urine of male stranger 1; UM2, urine of male stranger 2. *D*) Illustration of *Ptenα*$^{+/+}$ and *Ptenα*$^{\mu/\mu}$ mice brain gross morphology. Scale bar, 0.5 cm. *E*) Hematoxylin and eosin staining of sagittal brain sections of *Ptenα*$^{+/+}$ and *Ptenα*$^{\mu/\mu}$ mice. Scale bar: 2 mm (upper panel); 1 mm (lower panel). *F, G*) Immunofluorescence with anti-PGP9.5 (mitral cell marker, green) and DAPI (nucleus, blue) in sagittal sections of the OB from *Ptenα*$^{+/+}$ (*F*) and *Ptenα*$^{\mu/\mu}$ (*G*) mice. EPL, external plexiform layer; IPL, internal plexiform layer; MCL, mitral cell layer. Scale bar, 100 μm. *H*) Quantification of mitral cell number in *Ptenα*$^{+/+}$ and *Ptenα*$^{\mu/\mu}$ mice. Mice used are 4–6 mo old; n (*Ptenα*$^{+/+}$) = 6, n (*Ptenα*$^{\mu/\mu}$) = 7; $P < 0.0001$. *I*) BrdU incorporation and staining in *Ptenα*$^{+/+}$ and *Ptenα*$^{\mu/\mu}$ mice show newborn neurons in the OB and SVZ brain regions. Mice used are 4–6 mo old. DAPI, blue; BrdU, green. Scale bar, 200 μm. *J*) Quantification of BrdU^{+} cells in the granular cell layer of the OB in *Ptenα*$^{+/+}$ and *Ptenα*$^{\mu/\mu}$ mice. Mice used are 4–6 mo old; n (*Ptenα*$^{+/+}$) = 7, n (*Ptenα*$^{\mu/\mu}$) = 5. $P = 0.0238$. EV, ethyl vanillin. $^{*}P < 0.05$, $^{**}P < 0.01$, $^{***}P < 0.001$.

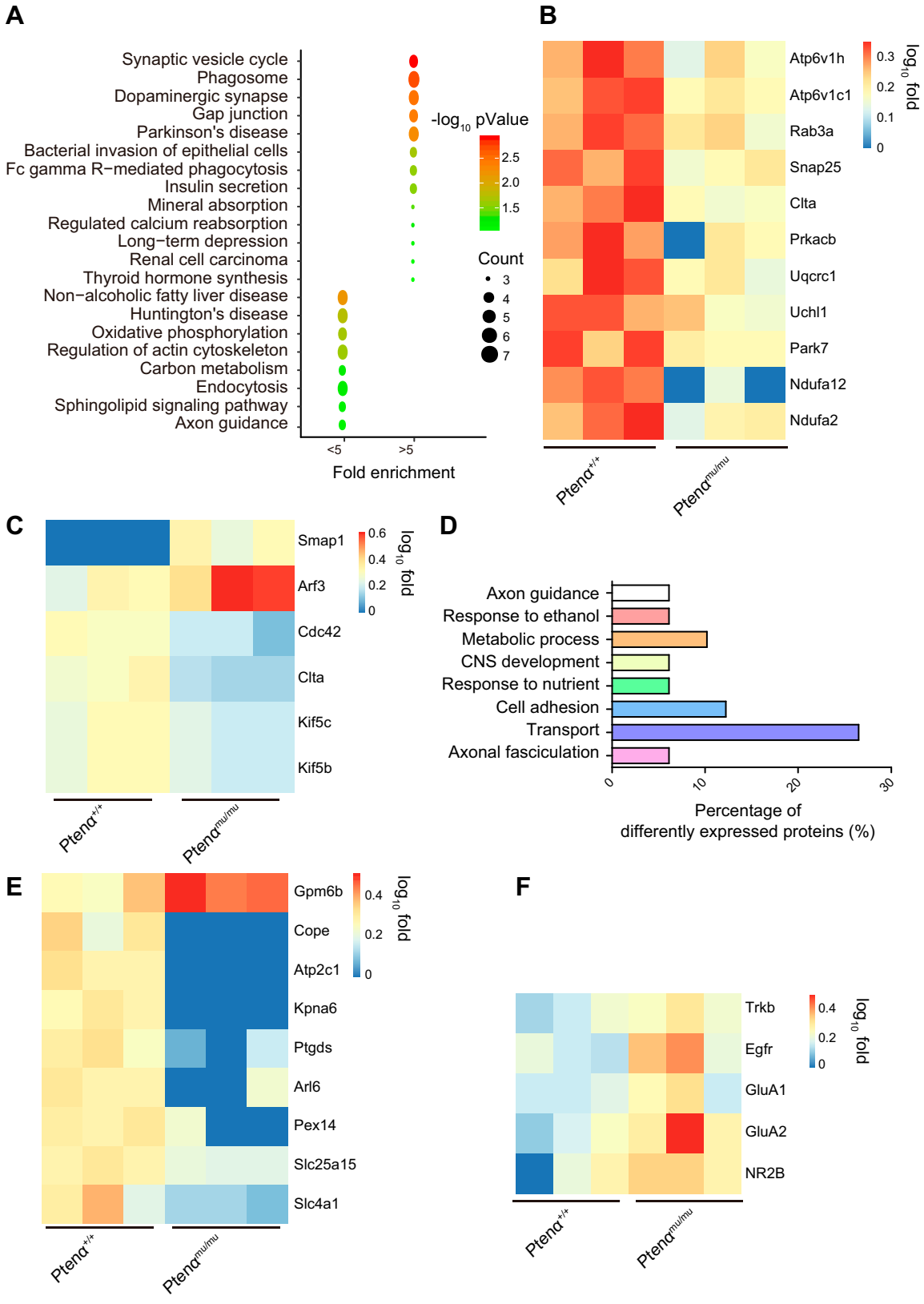

Figure 3. PTENα deletion in mice alters protein levels in pathways of synaptic vesicle cycle and endocytosis. *A–C*) Proteomic analysis of total OB lysate from *Ptenα*$^{+/+}$ and *Ptenα*$^{\mu/\mu}$ mice. Three-month-old mice, n = 3. Pathway enrichment analysis of proteomic results (*A*). Levels of differently expressed proteins identified in the synaptic vesicle cycling (*B*) and endocytic (*C*) pathway through proteomic quantification. *D–F*) Proteomic analysis of the membrane fraction from the OB from *Ptenα*$^{+/+}$ and *Ptenα*$^{\mu/\mu}$ mice. Three-month-old mice, n = 3. *D*) GO enrichment analysis of biologic processes of differentially expressed proteins. *E*) Levels of differentially expressed proteins involved in the transport pathway identified through proteomic quantification. *F*)

(*continued on next page*)

BIN1, and adaptor-related protein complex 2 subunit β1 (Ap2b1), and these proteins were not in the list of proteins pulled down by PTEN. Amphiphysin and BIN1 belong to the BAR domain family and are critical regulators in the process of clathrin-mediated endocytosis (CME) (13, 31, 32). Endocytosis has been demonstrated to be important in regulation of synaptic vesicle recycling, neuron migration, adhesion, differentiation, and survival (33).

Interaction between PTENα and amphiphysin or BIN1 was first confirmed by Western blotting pull-down samples from mouse OB tissue. Amphiphysin or BIN1 showed interaction with PTENα but not with PTEN (Fig. 4*C*; lane 2 *vs.* 3). Next, exogenous amphiphysin and PTENα or PTEN were coexpressed in HEK293T cells. Reciprocal IP demonstrated interaction of amphiphysin with PTENα (Fig. 4*D*; lane 2 *vs.* 1 and Fig. 4*E*; lane 2 *vs.* 1) but not with PTEN (Fig. 4*D*; lane 3). As reported, PTENα has an arginine-rich region and a putative membrane binding helix domain in the N-terminal extensional region, which may play a role in sustaining attachment of PTENα to the membrane (34). Our results demonstrate that both the arginine-rich region and the membrane binding helix domain are necessary for its interaction with amphiphysin (Supplemental Fig. S3*A*; lanes 2–3 *vs.* 1). It has been reported that stimulation with epidermal growth factor (EGF) promotes membrane association of the BAR domain (35). We confirmed EGFR expression in our HEK293T cells, and EGFR level is down-regulated upon EGF stimulation as previously reported by Hong *et al.* (36) (Supplemental Fig. S3*B*). It turns out that EGF stimulation abolishes interaction between PTENα and amphiphysin (Fig. 4*F*; lane 3 *vs.* 2). In addition, we found PTENα also interacts with BIN1 in HEK293T cells (Supplemental Fig. S3*C*, lane 2 *vs.* 1), which could form a heterodimer with amphiphysin as previously reported in refs. 37 and 38. However, this interaction is disrupted by overexpression of amphiphysin at the same time (Supplemental Fig. S3*D*; lane 3 *vs.* 2). As a subunit of assembly protein 2 complex, which is an important factor in the formation of clathrin-coated pits (CCPs), Ap2b1 has been reported to bind amphiphysin in the process of CME (38, 39). We also confirmed physical interaction of PTENα with Ap2b1 (Supplemental Fig. S3*E*). By cotransfecting with amphiphysin, we found that PTENα has a capability of binding amphiphysin similar to that of Ap2b1 (Supplemental Fig. S3*F*; lane 1 *vs.* 2). Fluorescent-tagged PTENα and amphiphysin were coexpressed in HEK293T cells, and colocalization of the proteins observed under confocal microscopy further confirmed their interaction (Supplemental Fig. S3*G*). Using total internal reflection fluorescence microscopy, we analyzed the lifetime of DsRED-tagged PTENα in endocytic pits and found that its membrane lifetime resembles the range of other CME components as previously reported by Ehrlich *et al.* (40) (Supplemental Fig. S3*H*). To determine whether PTENα regulates endocytosis *in vivo*, we evaluated the uptake of FITC-transferrin from medium in primary cultured *Ptenα*$^{+/+}$ and *Ptenα*$^{\mu/\mu}$ OB neurons (DIV10). After incubation in 50 ng/μl FITC-transferrin for 5 min at 37°C, cultured *Ptenα*$^{\mu/\mu}$ OB neurons showed significantly reduced levels of internalized transferrin (Fig. 4*G, H*). Previous studies have revealed surface receptors including EGFR and NR2B play important roles in postnatal neural development (11, 41). Up-regulation of EGFR and NR2B in OB membrane fraction identified by proteomic quantification was confirmed through Western blotting of cytosol and membrane fractions of *Ptenα*$^{+/+}$ and *Ptenα*$^{\mu/\mu}$ mice OB tissue (Fig. 4*I*; lane 4 *vs.* 3). Together, these results show that PTENα interacts with endocytic proteins and regulates endocytosis in OB neurons.

PTENα regulates endocytic protein assembly in a phosphatase activity–dependent manner

We found that the C2 domain and the phosphatase domain of PTENα are also important for its interaction with amphiphysin (**Fig. 5*A***; lanes 3–4 *vs.* 2). We were thus led to explore whether interaction between PTENα and amphiphysin is phosphorylation dependent. PTENα mutant C297S with disruption of both protein and lipid phosphatase activity abolished its binding to amphiphysin (Fig. 5*B*; lane 3 *vs.* 2), whereas PTENα G302E losing only lipid phosphatase activity showed similar interaction (Fig. 5*B*; lane 4 *vs.* 2). Amphiphysin has multiple *in vivo* phosphorylation sites, mostly on serine residues (42). When cotransfecting exogenous PTENα with amphiphysin, we found that total phosphorylated serine level in amphiphysin is significantly reduced (Fig. 5*C*). Through an *in vitro* phosphatase assay, purifying FLAG-tagged amphiphysin from HEK293T cells, mass spectrum analysis demonstrated that S268-phosphorylated peptide of amphiphysin showed significant reduction in intensity after incubation with purified PTENα as compared with control (Supplemental Table S1). We conducted o-immunoprecipitation (co-IP) analysis in HEK293T cells to confirm potential target sites of

Proteomic quantification of several surface receptors that are involved in neural differentiation and survival regulation and regulated by endocytosis. Arf3, ADP-ribosylation factor 3; Arl6, ADP-ribosylation factor-like protein 6; Atp2c1, calcium-transporting ATPase type 2C member 1; Atp6v1h, V-type proton ATPase subunit H; Atp6v1c1, V-type proton ATPase subunit C 1; Cdc42, cell division control protein 42; Clta, clathrin light chain A; Cope, coatomer subunit epsilon; GluA1, glutamate receptor 1; GluA2, glutamate receptor 2; Gpm6b, neuronal membrane glycoprotein M6-b; Kif5b, kinesin-1 heavy chain; Kif5c, kinesin heavy chain isoform 5C; Kpna6, importin subunit alpha-7; Ndufa2, NADH dehydrogenase 1 α subcomplex subunit 2; Ndufa12, NADH dehydrogenase 1 α subcomplex subunit 12; NR2B, glutamate receptor ionotropic, NMDA 2B; Park7, protein deglycase DJ-1; Pex14, peroxisomal membrane protein 14; Prkacb, cAMP-dependent protein kinase catalytic subunit beta; Ptgds, prostaglandin-H2 D-isomerase; Rab3a, Ras-related protein Rab-3A; Slc4a1, band 3 anion transport protein; Slc25a15, mitochondrial ornithine transporter 1; Smap1, stromal membrane-associated protein 1; Snap25, synaptosomal-associated protein 25; Trkb, BDNF/NT-3 growth factors receptor; UchIl, ubiquitin carboxyl-terminal hydrolase isozyme L1; Uqcrc1, cytochrome *b-c1* complex subunit 1.

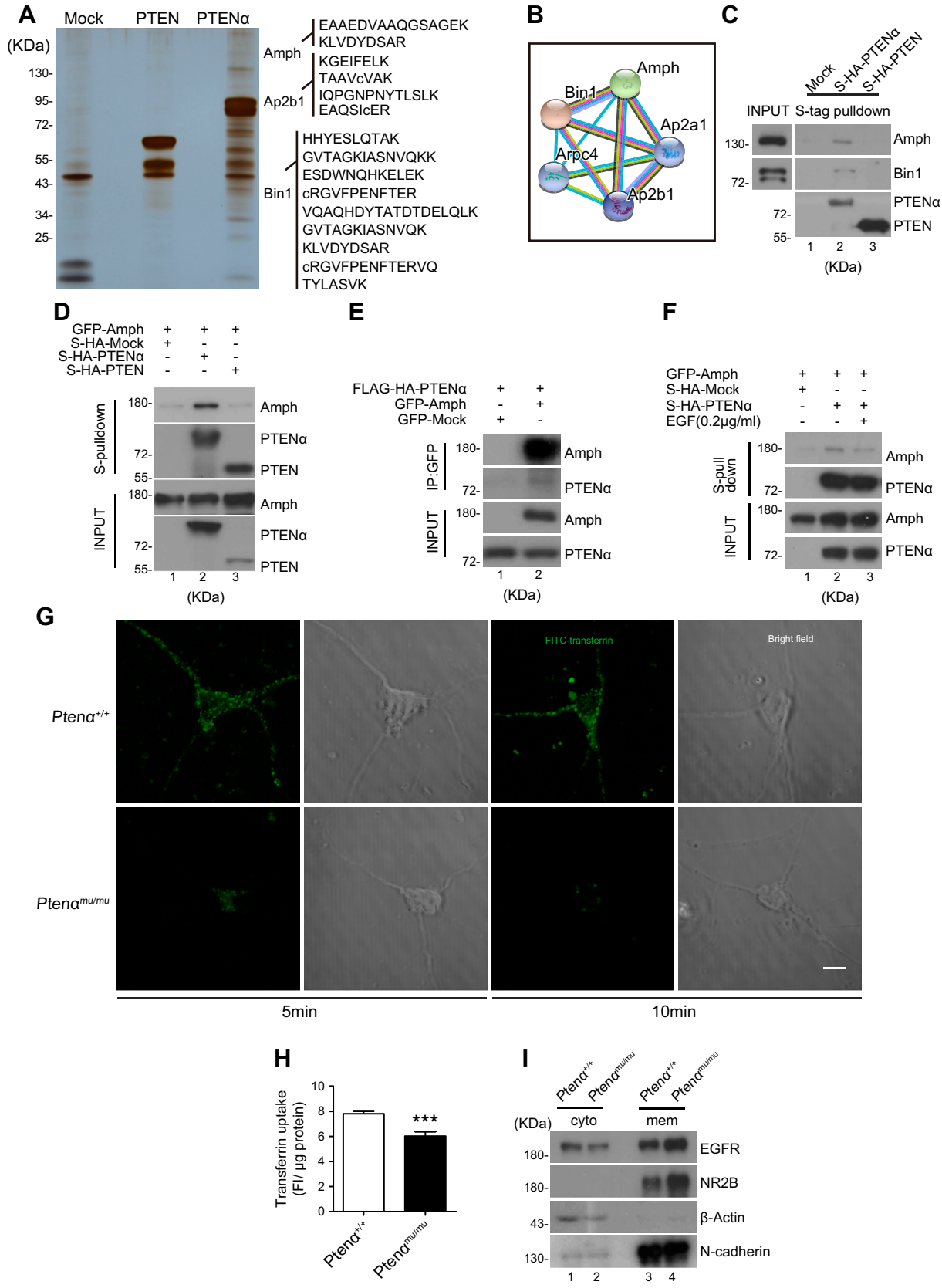

Figure 4. PTENα interacts with endocytic proteins and regulates endocytosis in OB neurons. *A*) Pull-down assays with PTENα and PTEN for identification of interacting proteins in mice OB. A group of mutually interacting endocytic proteins was specifically identified in the PTENα-interacting group. *B*) Illustration of PTENα-interacting endocytic proteins in the STRING protein interaction network (*https://string-db.org/*). *C*) Western blotting of Mock/PTEN/PTENα pull-down protein samples in mice OB tissue, confirming interaction of PTENα with endogenous amphiphysin and Bin1. *D–F*) Reciprocal IP of

(*continued on next page*)

PTENα phosphatase activity. Phosphorylation-null mutant amphiphysin S268A shows attenuated interaction (Fig. 5*D*; lane 4 *vs.* 1) and phosphomimetic mutant S268D shows enhanced interaction (Fig. 5*D*; lane 5 *vs.* 1) with PTENα. Four major phosphorylation sites of amphiphysin are S268, S272, S276, and S285 (42). By mutating the 4 sites simultaneously, we also identified attenuated interaction of PTENα with phosphorylation-null amphiphysin mutant and enhanced interaction with phosphomimetic mutant (Fig. 5*D*; lanes 2–3 *vs.* 1), further supporting that amphiphysin is a potential substrate of phosphatase PTENα.

Moreover, interaction between Ap2b1 and amphiphysin turns out to be stronger when PTENα is coexpressed (Fig. 5*E*; lane 2 *vs.* 1), and amphiphysin S268D showed reduced interaction with Ap2b1 compared with amphiphysin wild type or S268A when PTENα is coexpressed (Fig. 5*F*; lane 4 *vs.* 2–3). IP tests in *Ptenα*$^{+/+}$ and *Ptenα*$^{\mu/\mu}$ OB tissue showed that interaction between amphiphysin and Ap2b1 *in vivo* is impaired when PTENα is deleted (Fig. 5*G*; lane 2 *vs.* 1). It has been reported that phosphorylation of amphiphysin impairs its interaction with Ap2b1 and negatively regulates endocytosis (43–45). Our data show that coexpression of PTENα may facilitate interaction between amphiphysin and Ap2b1 by functioning as an adaptor for their interaction through dephosphorylating amphiphysin S268, and loss of PTENα *in vivo* attenuates amphiphysin-Ap2b1 interaction. Figure 5*H* provides a graphic illustration of our hypothesis on the molecular mechanism that PTENα is involved in regulation of endocytosis.

To further test whether the impaired amphiphysin-Ap2b1 interaction in *Ptenα*$^{\mu/\mu}$ mice accounts for olfactory dysfunction, we tried to rescue amphiphysin-Ap2b1 interaction by intraperitoneal administration of PD98059. PD98059 is known as an inhibitor of MAPKK and has been previously reported by Shang *et al.* (45) to prevent amphiphysin-Ap2b1 dissociation in PC3 cells by inhibiting phosphorylation of amphiphysin. We found that PD98059 treatment for 3 h in *Ptenα*$^{\mu/\mu}$ mice can rescue amphiphysin-Ap2b1 interaction (Supplemental Fig. S4*A*). Odor sensitivity of *Ptenα*$^{\mu/\mu}$ mice is also rescued after PD98059 administration (Supplemental Fig. S4*B*).

Collectively, our results show that PTENα interacts with CME components, regulates CME complex assembly dependent of its phosphatase activity, and influences endocytosis in the OB, which might account for the olfactory dysfunction of PTENα deficiency.

Mutations located in the PTENα N-terminal extensional region are identified in patients with neurodegenerative diseases manifested with early olfactory loss

Early symptoms of olfactory dysfunction are strongly correlated with multiple types of neurodegenerative disorders, including idiopathic PD, LBD, vascular dementia, frontotemporal dementia, and multiple sclerosis (2). In order to determine whether there is a correlation between PTENα and diseases that manifest early olfactory dysfunction, we collected 40 blood samples of patients with these neurodegenerative disorders and extracted genomic DNA for sequencing. To search for PTENα mutation, we sequenced 519 nt of its N-terminal extensional region. Detailed information regarding samples used is listed in Supplemental Table S2. As illustrated in **Fig. 6*A*, *B***, we found the mutation H169N (c.505C > A) in a patient with PD and mutation Y123C (c.368A > G) in a patient with LBD. No mutation of either of these 2 sites was found in DNA samples from normal individuals. Based on our findings that PTENα is involved in endocytosis, we wondered whether these mutations could impact the association between PTENα and endocytic proteins. According to our results, PTENα mutants only showed slightly weakened interaction with amphiphysin (Fig. 6*C*; lanes 3–4 *vs.* 2). However, the PTENα Y123C mutant dampened its ability to facilitate binding of amphiphysin to Ap2b1 (Fig. 6*D*; lane 3 *vs.* 2), and PTENα H169N showed increased ability to facilitate binding of amphiphysin to Ap2b1 (Fig. 6*C*; lane 4 *vs.* 2).

To determine whether PTENα H169N is directly related to olfactory function, we injected adeno-associated virus (AAV) overexpressing PTENα or PTENα H169N into OBs of wild-type mice and conducted behavioral tests after 4 mo to evaluate olfactory function. Figure 6*E* shows expression of injected AAV by Western blotting different brain regions. We found that even though mice with PTENα H169N overexpression in OB showed no obvious effect on general olfactory function compared with wild-type PTENα (Fig. 6*F*), these animals demonstrated impaired odor sensitivity (Fig. 6*G*), providing more direct evidence linking PTENα H169N and olfactory function. Further experiments through immunostaining with mitral cell marker PGP9.5 and confocal microscopy detected no difference on morphology (Fig. 6*H*). Together, these results

exogenously expressed proteins in HEK293T cells. *S*-HA–tagged PTEN or PTENα was pulled down by *S*-tag agarose, and protein complexes were immunoblotted with GFP antibody for evaluation of GFP-tagged amphiphysin (*D*). HEK293T cells were cotransfected with GFP-tagged amphiphysin and HA-FLAG–tagged PTENα, immunoprecipitated with GFP antibody and immunoblotted with HA antibody for evaluation of HA-FLAG–tagged PTENα (*E*) *S*-HA–tagged PTENα and GFP-tagged amphiphysin were cotransfected in HEK293T cells, followed by treatment with 0.2 μg/ml EGF for 15 min or no treatment. The cells were then lysed, subjected to *S*-protein pull-down, and immunoblotted with GFP antibody (*F*). *G*) Confocal imaging of primary cultured *Ptenα*$^{+/+}$ and *Ptenα*$^{\mu/\mu}$ OB neurons (DIV10) after incubation in 50 ng/μl FITC-transferrin for 5 or 10 min at 37°C. Scale bar, 10 μm. *H*) *Ptenα*$^{+/+}$ and *Ptenα*$^{\mu/\mu}$ OB neurons cultured in 96-well plates were lysed after incubation in 50 ng/μl FITC-transferrin for 5 min at 37°C at DIV10, and fluorescent intensity of 520 nm (excited at 490 nm) and protein concentration were determined using a microplate reader for statistical analysis; n (*Ptenα*$^{+/+}$) = 29, n (*Ptenα*$^{\mu/\mu}$) = 19; $P < 0.0001$. *I*) Western blotting of cytosol (cyto) and membrane fraction (mem) of *Ptenα*$^{+/+}$ and *Ptenα*$^{\mu/\mu}$ mouse OB tissue for confirmation of surface receptor protein levels. β-Actin is shown as a cytosol protein control, and *N*-cadherin is shown as a membrane protein control. Amph, amphiphysin. ***$P < 0.001$.

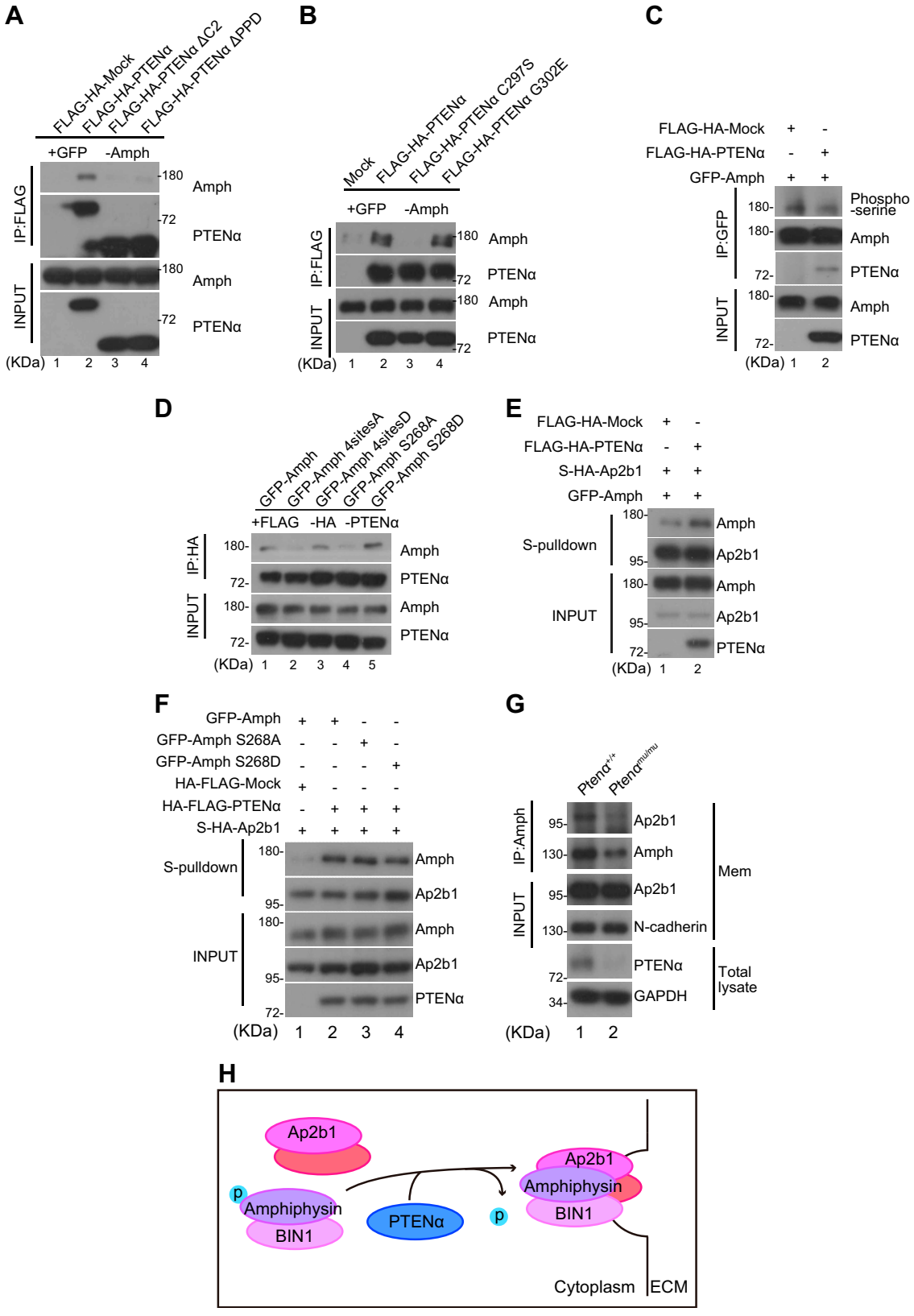

Figure 5. PTENα regulates endocytic protein assembly in a phosphatase activity–dependent manner. *A*) Co-IP analysis of different PTENα truncations with GFP-tagged amphiphysin. ΔC2, C2 domain deleted; ΔPPD, phosphatase domain deleted. *B*) Co-IP analysis of PTENα mutant C297S, G302E, or PTENα wild type with GFP-tagged amphiphysin in HEK293T cells. The cells were lysed and immunoprecipitated with FLAG antibody and immunoblotted with GFP antibody for evaluation of GFP-tagged amphiphysin. *C*) GFP-tagged amphiphysin was cotransfected with Mock or FLAG-HA–tagged PTENα in HEK293T cells, immunoprecipitated with GFP antibody, and immunoblotted with anti-phosphoserine to evaluate total phosphorylated serine

(*continued on next page*)

show that PTENα mutants identified in neurodegenerative diseases with olfactory dysfunction disrupt interaction of amphiphysin-Ap2b1, and overexpression of PTENα H169N in OB of wild-type mice disrupts olfactory function.

DISCUSSION

Different roles that PTEN and PTENα play in brain

PTEN is well known as a tumor suppressor, but at the same time, its involvement in neurologic disorders and underlying mechanisms has also been extensively studied. PTEN has been linked to multiple neurologic disorders, such as seizure, autism, ataxia, AD, and PD (46). Moreover, it has been reported to play different roles at different stages of brain development, including neuron differentiation, migration, and synaptic plasticity modulation, mostly depending on its regulation on downstream target Akt (47, 48).

PTENα is recently shown to play a diversity of biologic roles in several recent studies, including regulation of mitochondria metabolism (21), regulation of spatial learning and contextual fear memory (22), cardiac homeostasis maintenance and regulation of mitophagy (23, 24), and regulation of type I IFN responses and antiviral immunity (25). PTENα is expressed in many types of tissue, and expression of PTENα in the brain is high. Moreover, we found the level of PTENα expression in the OB is obviously higher as compared with other regions of the brain, which has incited our interest in exploration of the role PTENα plays in olfaction.

Recently, PTEN is also shown to play a role in regulation of CCP dynamics. PTEN regulates the proportion of short-lived CCPs depending on its lipid phosphatase activity (49). According to our study, PTENα is involved in CME regulation by interacting with amphiphysin depending on its protein phosphatase activity. PTENα and amphiphysin are both highly expressed in brain, which provides the basis for the function of PTENα on CME in brain. However, what role PTENα may play in CME in other systems remains to be explored.

Role of PTENα in olfactory deficits in neurodegenerative diseases

Olfactory dysfunction is common in an aging population. A study from a decade ago by Murphy *et al.* (3) showed that the prevalence of measured olfactory impairment was 24.5%, and this number increased with age. Moreover, olfaction loss is an early symptom of many types of neurologic disease such as schizophrenia, PD, and AD. Approximately 90% of patients with AD and PD develop early symptoms of olfactory loss (1). To explore the possible relevance of PTENα to human diseases with olfactory dysfunction, we sequenced genomic DNA from patients with several neurodegenerative diseases related with early symptoms of olfactory dysfunction. Two mutation sites in the N-terminal extension region of PTENα were identified. According to the Genome Aggregation Database (gnomAD; *https://gnomad.broadinstitute.org/*), the allele frequencies of the mutations regarding Y123C and H169N in general population of East Asia are 0.001282 (2/1560) and 0 (0/18394), respectively. We identified differences in protein interaction between PTENα wild-type and counterpart mutant proteins through mass spectrometry analysis. The differentially interacting proteins showed diversity in biologic processes through enrichment analysis, reflecting the complexity of the mechanisms that may involve PTENα mutants.

Investigating olfactory function in PTENα-deficient mice, we found impaired food-finding ability and loss of mitral cells in the OB. Previous studies demonstrated that patients with PD showed a significant decrease of mitral/tufted cells in the OB compared with controls (50), similar to what we found in mice deficient in PTENα.

Endocytosis and neural development

Earlier studies illustrated the important role played by endocytosis in neural development in several ways. First, precise and elaborate regulation of quantity and location of surface receptors through endocytosis is critical for normal neural development during processes of neuritogenesis and axonal guidance (11). In adult OB, a large number of newborn cells are generated every day, and a large proportion of these fail to survive because of unsuccessful establishment of connectivity. Endocytic regulation in the OB is therefore even more important. Secondly, endocytosis of receptors can also regulate downstream signaling and influence neural development. The results of our OB membrane proteomic analysis also revealed extensive differences in protein expression in axon guidance, protein transport, cell adhesion, CNS development, and so on. These differences in protein expression in the OB membrane may be a result of alteration of endocytosis.

level of amphiphysin. *D*) GFP-tagged amphiphysin or mutant was cotransfected with FLAG-HA–tagged PTENα in HEK293T cells, immunoprecipitated with HA antibody, and immunoblotted with GFP antibody to evaluate GFP-tagged amphiphysin. *E*) *S*-HA–tagged Ap2b1 was pulled down by *S*-tag agarose, and protein complexes were immunoblotted with GFP antibody to evaluate for GFP-tagged amphiphysin when FLAG-HA–tagged PTENα was cotransfected or not cotransfected. *F*) *S*-HA–tagged Ap2b1 was pulled down by *S*-tag agarose, and protein complexes were immunoblotted with GFP antibody to evaluate for GFP-tagged amphiphysin or mutants when FLAG-HA–tagged PTENα was cotransfected (lanes 2–4) or mock was cotransfected (lane 1). *G*) Amphiphysin was immunoprecipitated from membrane fraction (Mem) of *Ptenα*$^{+/+}$ and *Ptenα*$^{\mu/\mu}$ mice OB tissue, and the proteins were immunoblotted with Ap2b1 antibody for interaction evaluation. *H*) Schematic model illustrating involvement of PTENα in regulation of endocytic proteins. PTENα dephosphorylates amphiphysin and increases interaction between amphiphysin and Ap2b1 to facilitate endocytosis. Amph, amphiphysin.

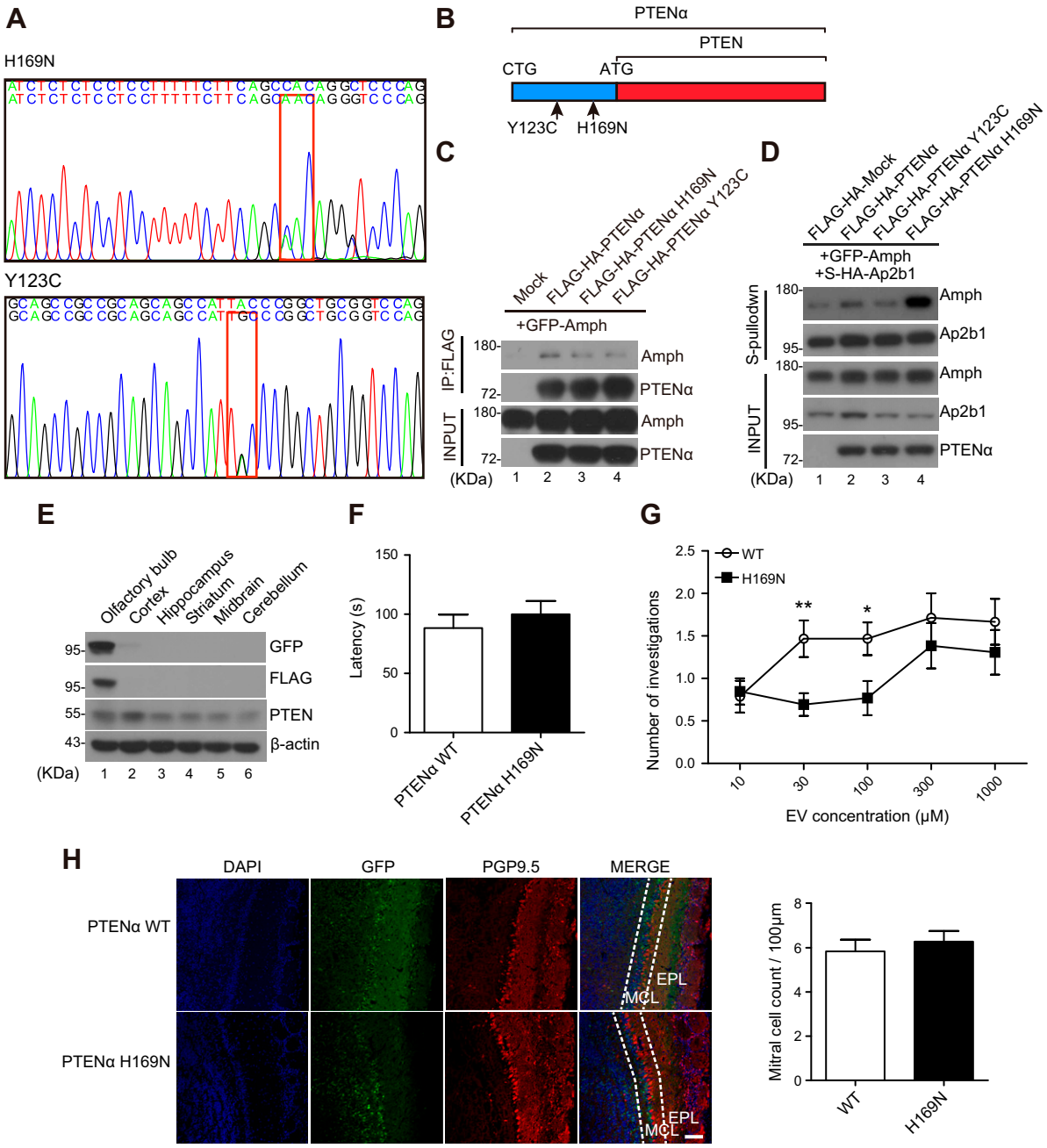

Figure 6. Mutations located in PTENα N-terminal extensional regions are identified in patients with neurodegenerative diseases highly relevant to olfactory loss, and exogenous expression of PTENα mutant H169N in wild-type mice impairs odor sensitivity. *A*) Mutation H169N is identified in a patient with PD (upper panel), and Y123C is identified in a patient with LBD (lower panel). *B*) Schematic representations of locations of the identified mutations. *C*) FLAG-HA–tagged PTENα or PTENα mutant was coexpressed with GFP-tagged amphiphysin in HEK293T cells and immunoprecipitated with FLAG antibody, and protein complexes were immunoblotted with GFP antibody to identify GFP-tagged amphiphysin. *D*) *S*-HA–tagged Ap2b1 was pulled down by *S*-tag agarose, and protein complexes were immunoblotted with GFP antibody to evaluate for GFP-tagged amphiphysin when FLAG-HA–tagged PTENα or PTENα mutant was cotransfected. *E*) Evaluation of expression of GFP-FLAG–PTENα in mice subjected to AAV injection into OBs by Western blotting brain tissue lysate of different regions. *F*) Buried food pellet test of mice subjected to AAV injection into OBs overexpressing PTENα ($n = 15$) or PTENα H169N ($n = 13$). *G*) Odor sensitivity tests of mice subjected to AAV injection into OBs overexpressing PTENα ($n = 15$) or PTENα H169N ($n = 13$). EV, ethyl vanillin; $P = 0.0089$. *H*) Immunofluorescence with anti-PGP9.5 (mitral cell marker, green) and DAPI (nucleus, blue) in OB sections from mice injected by AAV overexpressing PTENα or PTENα H169N and quantification of PGP9.5 in the 2 groups. Scale bar, 100 μm; $n = 10$. $P = 0.5421$. Amph, amphiphysin; EPL, external plexiform layer; MCL, mitral cell layer; WT, wild type. $^*P < 0.05$, $^{**}P < 0.01$.

Results of our pull-down assay show that PTENα interacts with proteins involved in CME. Proteomic analysis of *Ptenα*$^{+/+}$ and *Ptenα*$^{\mu/\mu}$ OB show protein alteration in the pathway of endocytosis as well. For example, ADP-ribosylation factor 3 and small ADP-ribosylation factor GTPase-activating protein 1, proteins involved in transferrin recycling to the plasma membrane (51) and transferrin receptor endocytosis (52), show elevated

protein level in *Ptenα*$^{\mu/\mu}$ OB tissue, which is possibly a compensatory mechanism of endocytic deficiency. Downregulation of clathrin light chain A in *Ptenα*$^{\mu/\mu}$ OB tissue indicates that it might be a direct or indirect target regulated by PTENα. Glycoprotein M6B was previously shown to regulate trafficking of the serotonin transporter (53), and its elevation in membrane fraction of *Ptenα*$^{\mu/\mu}$ OB tissue might also be the compensatory outcome of endocytic deficiency. Elevated levels of receptors such as EGFR that mediate critical signaling pathways of neural development and activation are also observed in the membrane fraction of *Ptenα*$^{\mu/\mu}$ OB.

Collectively, we propose PTENα may play an important role in sustaining an appropriate level of receptor signaling through endocytic regulation, thereby affecting neural development and establishment of neural circuits in adult OB and maintaining normal olfactory function. Whereas deletion of PTENα results in attenuated amphiphysin-Ap2b1 interaction and reduced endocytosis in the OB, thereby resulting in disturbance of neural circuit establishment and olfactory dysfunction, overexpression of PTENα mutant H169N in mice OB disrupts olfactory function, further supporting the conclusion that PTENα is involved in regulation of olfaction.

Taken together, our work demonstrates a novel function of the newly identified protein PTENα in regulation of endocytosis and reveals the involvement of PTENα in olfactory processes in mouse models and human patients. Disabilities in odor perception have been regarded as an approach of early screening for several types of neurodegenerative diseases such as PD. Our work has provided new insight into mechanisms of olfactory deterioration in neurodegenerative diseases, offering a potential marker for clinical diagnosis and a novel potential therapeutic target. FJ

ACKNOWLEDGMENTS

The authors thank X. Meng (Peking University Health Science Center) for genomic DNA extraction from blood samples, Jia Liu (Peking University Health Science Center) for neurotransmitter quantification by liquid chromatography with tandem mass spectrometry (LC-MS-MS), and L. Liang (Peking University Health Science Center) for protein expression and purification from Sf9 cells. This work was supported by grants to Y.Y., including the National Key Research and Development Program of China (Grant 2016YFA0500302), the National Natural Science Foundation of China (Grants 81430056, 31420103905, and 81372491), the Beijing Natural Science Foundation (Key Grant 7161007), and the Lam Chung Nin Foundation for Systems Biomedicine. P.W. was supported by the National Natural Scientific Foundation of China (Grant 31800849). The authors declare no conflicts of interest.

AUTHOR CONTRIBUTIONS

Y. Yuan and Y. Yin conceived the study and designed the major experiments; Y. Yuan performed the majority of the experiments and data analysis; Y. Yuan and P. Wang performed behavioral examination and AAV injection; F. Mei collected blood samples and provided DNA samples Y. Yuan, X. Zhao, J. Zhou, and Y. Jin performed sample preparation for proteomics and data analysis; and Y. Yuan, M. A. McNutt, and Y. Yin wrote the manuscript.

REFERENCES

1. Doty, R. L. (2012) Olfactory dysfunction in Parkinson disease. *Nat. Rev. Neurol.* **8**, 329–339
2. Doty, R. L. (2017) Olfactory dysfunction in neurodegenerative diseases: is there a common pathological substrate? *Lancet Neurol.* **16**, 478–488
3. Murphy, C., Schubert, C. R., Cruickshanks, K. J., Klein, B. E., Klein, R., and Nondahl, D. M. (2002) Prevalence of olfactory impairment in older adults. *JAMA* **288**, 2307–2312
4. Kovács, T. (2004) Mechanisms of olfactory dysfunction in aging and neurodegenerative disorders. *Ageing Res. Rev.* **3**, 215–232
5. Doty, R. L. (2008) The olfactory vector hypothesis of neurodegenerative disease: is it viable? *Ann. Neurol.* **63**, 7–15
6. Ge, S., Goh, E. L., Sailor, K. A., Kitabatake, Y., Ming, G. L., and Song, H. (2006) GABA regulates synaptic integration of newly generated neurons in the adult brain. *Nature* **439**, 589–593
7. Berg, D. A., Belnoue, L., Song, H., and Simon, A. (2013) Neurotransmitter-mediated control of neurogenesis in the adult vertebrate brain. *Development* **140**, 2548–2561
8. Mombaerts, P. (2004) Genes and ligands for odorant, vomeronasal and taste receptors. *Nat. Rev. Neurosci.* **5**, 263–278
9. Bear, D. M., Lassance, J. M., Hoekstra, H. E., and Datta, S. R. (2016) The evolving neural and genetic architecture of vertebrate olfaction. *Curr. Biol.* **26**, R1039–R1049
10. Kawauchi, T. (2012) Cell adhesion and its endocytic regulation in cell migration during neural development and cancer metastasis. *Int. J. Mol. Sci.* **13**, 4564–4590
11. Tojima, T., Itofusa, R., and Kamiguchi, H. (2010) Asymmetric clathrin-mediated endocytosis drives repulsive growth cone guidance. *Neuron* **66**, 370–377
12. Tojima, T., Itofusa, R., and Kamiguchi, H. (2014) Steering neuronal growth cones by shifting the imbalance between exocytosis and endocytosis. *J. Neurosci.* **34**, 7165–7178
13. Wu, Y., Matsui, H., and Tomizawa, K. (2009) Amphiphysin I and regulation of synaptic vesicle endocytosis. *Acta Med. Okayama* **63**, 305–323
14. Sekiguchi, M., Katayama, S., Hatano, N., Shigeri, Y., Sueyoshi, N., and Kameshita, I. (2013) Identification of amphiphysin 1 as an endogenous substrate for CDKL5, a protein kinase associated with X-linked neurodevelopmental disorder. *Arch. Biochem. Biophys.* **535**, 257–267
15. Trempe, J. F., Chen, C. X., Grenier, K., Camacho, E. M., Kozlov, G., McPherson, P. S., Gehring, K., and Fon, E. A. (2009) SH3 domains from a subset of BAR proteins define a Ubl-binding domain and implicate parkin in synaptic ubiquitination. *Mol. Cell* **36**, 1034–1047
16. Miller, D. T., Adam, M. P., Aradhya, S., Biesecker, L. G., Brothman, A. R., Carter, N. P., Church, D. M., Crolla, J. A., Eichler, E. E., Epstein, C. J., Faucett, W. A., Feuk, L., Friedman, J. M., Hamosh, A., Jackson, L., Kaminsky, E. B., Kok, K., Krantz, I. D., Kuhn, R. M., Lee, C., Ostell, J. M., Rosenberg, C., Scherer, S. W., Spinner, N. B., Stavropoulos, D. J., Tepperberg, J. H., Thorland, E. C., Vermeesch, J. R., Waggoner, D. J., Watson, M. S., Martin, C. L., and Ledbetter, D. H. (2010) Consensus statement: chromosomal microarray is a first-tier clinical diagnostic test for individuals with developmental disabilities or congenital anomalies. *Am. J. Hum. Genet.* **86**, 749–764
17. Hsiao, S. J., Karajannis, M. A., Diolaiti, D., Mansukhani, M. M., Bender, J. G., Kung, A. L., and Garvin, J. H., Jr. (2017) A novel, potentially targetable TMEM106B-BRAF fusion in pleomorphic xanthoastrocytoma. *Cold Spring Harb. Mol. Case Stud.* **3**, a001396
18. Kaminsky, E. B., Kaul, V., Paschall, J., Church, D. M., Bunke, B., Kunig, D., Moreno-De-Luca, D., Moreno-De-Luca, A., Mulle, J. G., Warren, S. T., Richard, G., Compton, J. G., Fuller, A. E., Gliem, T. J., Huang, S., Collinson, M. N., Beal, S. J., Ackley, T., Pickering, D. L., Golden, D. M., Aston, E., Whitby, H., Shetty, S., Rossi, M. R., Rudd, M. K., South, S. T., Brothman, A. R., Sanger, W. G., Iyer, R. K., Crolla, J. A., Thorland, E. C., Aradhya, S., Ledbetter, D. H., and Martin, C. L. (2011) An evidence-based approach to establish the functional and clinical significance of copy number variants in intellectual and developmental disabilities. *Genet. Med.* **13**, 777–784

19. Di Paolo, G., Sankaranarayanan, S., Wenk, M. R., Daniell, L., Perucco, E., Caldarone, B. J., Flavell, R., Picciotto, M. R., Ryan, T. A., Cremona, O., and De Camilli, P. (2002) Decreased synaptic vesicle recycling efficiency and cognitive deficits in amphiphysin 1 knockout mice. *Neuron* **33**, 789–804
20. Hopkins, B. D., Fine, B., Steinbach, N., Dendy, M., Rapp, Z., Shaw, J., Pappas, K., Yu, J. S., Hodakoski, C., Mense, S., Klein, J., Pegno, S., Sulis, M. L., Goldstein, H., Amendolara, B., Lei, L., Maurer, M., Bruce, J., Canoll, P., Hibshoosh, H., and Parsons, R. (2013) A secreted PTEN phosphatase that enters cells to alter signaling and survival. *Science* **341**, 399–402
21. Liang, H., He, S., Yang, J., Jia, X., Wang, P., Chen, X., Zhang, Z., Zou, X., McNutt, M. A., Shen, W. H., and Yin, Y. (2014) PTENα, a PTEN isoform translated through alternative initiation, regulates mitochondrial function and energy metabolism. *Cell Metab.* **19**, 836–848
22. Wang, P., Mei, F., Hu, J., Zhu, M., Qi, H., Chen, X., Li, R., McNutt, M. A., and Yin, Y. (2017) PTENα modulates CaMKII signaling and controls contextual fear memory and spatial learning. *Cell Reports* **19**, 2627–2641
23. Li, G., Yang, J., Yang, C., Zhu, M., Jin, Y., McNutt, M. A., and Yin, Y. (2018) PTENα regulates mitophagy and maintains mitochondrial quality control. *Autophagy* **14**, 1742–1760
24. Wang, L., Cho, Y. L., Tang, Y., Wang, J., Park, J. E., Wu, Y., Wang, C., Tong, Y., Chawla, R., Zhang, J., Shi, Y., Deng, S., Lu, G., Wu, Y., Tan, H. W., Pawijit, P., Lim, G. G., Chan, H. Y., Zhang, J., Fang, L., Yu, H., Liou, Y. C., Karthik, M., Bay, B. H., Lim, K. L., Sze, S. K., Yap, C. T., and Shen, H. M. (2018) PTEN-L is a novel protein phosphatase for ubiquitin dephosphorylation to inhibit PINK1-Parkin-mediated mitophagy. *Cell Res.* **28**, 787–802; erratum: 872–873
25. Cao, Y., Wang, H., Yang, L., Zhang, Z., Li, C., Yuan, X., Bu, L., Chen, L., Chen, Y., Li, C. M., and Guo, D. (2018) PTEN-L promotes type I interferon responses and antiviral immunity. *Cell. Mol. Immunol.* **15**, 48–57
26. Daynac, M., Morizur, L., Chicheportiche, A., Mouthon, M. A., and Boussin, F. D. (2016) Age-related neurogenesis decline in the subventricular zone is associated with specific cell cycle regulation changes in activated neural stem cells. *Sci. Rep.* **6**, 21505
27. Suh, H., Deng, W., and Gage, F. H. (2009) Signaling in adult neurogenesis. *Annu. Rev. Cell. Dev. Biol.* **25**, 253–275
28. Yamaguchi, M., and Mori, K. (2005) Critical period for sensory experience-dependent survival of newly generated granule cells in the adult mouse olfactory bulb. *Proc. Natl. Acad. Sci. USA* **102**, 9697–9702
29. Rochefort, C., Gheusi, G., Vincent, J. D., and Lledo, P. M. (2002) Enriched odor exposure increases the number of newborn neurons in the adult olfactory bulb and improves odor memory. *J. Neurosci.* **22**, 2679–2689
30. Corotto, F. S., Henegar, J. R., and Maruniak, J. A. (1994) Odor deprivation leads to reduced neurogenesis and reduced neuronal survival in the olfactory bulb of the adult mouse. *Neuroscience* **61**, 739–744
31. Meinecke, M., Boucrot, E., Camdere, G., Hon, W. C., Mittal, R., and McMahon, H. T. (2013) Cooperative recruitment of dynamin and BIN/amphiphysin/Rvs (BAR) domain-containing proteins leads to GTP-dependent membrane scission. *J. Biol. Chem.* **288**, 6651–6661
32. Suetsugu, S., Kurisu, S., and Takenawa, T. (2014) Dynamic shaping of cellular membranes by phospholipids and membrane-deforming proteins. *Physiol. Rev.* **94**, 1219–1248
33. Saheki, Y., and De Camilli, P. (2012) Synaptic vesicle endocytosis. *Cold Spring Harb. Perspect. Biol.* **4**, a005645
34. Masson, G. R., Perisic, O., Burke, J. E., and Williams, R. L. (2016) The intrinsically disordered tails of PTEN and PTEN-L have distinct roles in regulating substrate specificity and membrane activity. *Biochem. J.* **473**, 135–144
35. Zhao, X., Wang, D., Liu, X., Liu, L., Song, Z., Zhu, T., Adams, G., Gao, X., Tian, R., Huang, Y., Chen, R., Wang, F., Liu, D., Yu, X., Chen, Y., Chen, Z., Teng, M., Ding, X., and Yao, X. (2013) Phosphorylation of the Bin, Amphiphysin, and RSV161/167 (BAR) domain of ACAP4 regulates membrane tubulation. *Proc. Natl. Acad. Sci. USA* **110**, 11023–11028
36. Hong, S. Y., Shih, Y. P., Li, T., Carraway III, K. L., and Lo, S. H. (2013) CTEN prolongs signaling by EGFR through reducing its ligand-induced degradation. *Cancer Res.* **73**, 5266–5276
37. Wigge, P., Köhler, K., Vallis, Y., Doyle, C. A., Owen, D., Hunt, S. P., and McMahon, H. T. (1997) Amphiphysin heterodimers: potential role in clathrin-mediated endocytosis. *Mol. Biol. Cell* **8**, 2003–2015
38. Wigge, P., and McMahon, H. T. (1998) The amphiphysin family of proteins and their role in endocytosis at the synapse. *Trends Neurosci.* **21**, 339–344
39. Slepnev, V. I., Ochoa, G. C., Butler, M. H., and De Camilli, P. (2000) Tandem arrangement of the clathrin and AP-2 binding domains in amphiphysin 1 and disruption of clathrin coat function by amphiphysin fragments comprising these sites. *J. Biol. Chem.* **275**, 17583–17589
40. Ehrlich, M., Boll, W., Van Oijen, A., Hariharan, R., Chandran, K., Nibert, M. L., and Kirchhausen, T. (2004) Endocytosis by random initiation and stabilization of clathrin-coated pits. *Cell* **118**, 591–605
41. Ayuso-Sacido, A., Moliterno, J. A., Kratovac, S., Kapoor, G. S., O'Rourke, D. M., Holland, E. C., García-Verdugo, J. M., Roy, N. S., and Boockvar, J. A. (2010) Activated EGFR signaling increases proliferation, survival, and migration and blocks neuronal differentiation in post-natal neural stem cells. *J. Neurooncol.* **97**, 323–337
42. Craft, G. E., Graham, M. E., Bache, N., Larsen, M. R., and Robinson, P. J. (2008) The *in vivo* phosphorylation sites in multiple isoforms of amphiphysin I from rat brain nerve terminals. *Mol. Cell. Proteomics* **7**, 1146–1161
43. Cousin, M. A., and Robinson, P. J. (2001) The dephosphins: dephosphorylation by calcineurin triggers synaptic vesicle endocytosis. *Trends Neurosci.* **24**, 659–665
44. Floyd, S. R., Porro, E. B., Slepnev, V. I., Ochoa, G. C., Tsai, L. H., and De Camilli, P. (2001) Amphiphysin 1 binds the cyclin-dependent kinase (cdk) 5 regulatory subunit p35 and is phosphorylated by cdk5 and cdc2. *J. Biol. Chem.* **276**, 8104–8110
45. Shang, W. H., Adachi, Y., Nakamura, A., Copeland, T., Kim, S. R., and Kamata, T. (2004) Regulation of amphiphysin1 by mitogen-activated protein kinase: its significance in nerve growth factor receptor-mediated endocytosis. *J. Biol. Chem.* **279**, 40890–40896
46. Kreis, P., Leondaritis, G., Lieberam, I., and Eickholt, B. J. (2014) Subcellular targeting and dynamic regulation of PTEN: implications for neuronal cells and neurological disorders. *Front. Mol. Neurosci.* **7**, 23
47. Williams, M. R., DeSpenza, T., Jr., Li, M., Gulledge, A. T., and Luikart, B. W. (2015) Hyperactivity of newborn Pten knock-out neurons results from increased excitatory synaptic drive. *J. Neurosci.* **35**, 943–959
48. Amiri, A., Cho, W., Zhou, J., Birnbaum, S. G., Sinton, C. M., McKay, R. M., and Parada, L. F. (2012) Pten deletion in adult hippocampal neural stem/progenitor cells causes cellular abnormalities and alters neurogenesis. *J. Neurosci.* **32**, 5880–5890
49. Rosselli-Murai, L. K., Yates, J. A., Yoshida, S., Bourg, J., Ho, K. K. Y., White, M., Prisby, J., Tan, X., Altemus, M., Bao, L., Wu, Z. F., Veatch, S. L., Swanson, J. A., Merajver, S. D., and Liu, A. P. (2018) Loss of PTEN promotes formation of signaling-capable clathrin-coated pits. *J. Cell Sci.* **131**, jcs208926
50. Cave, J. W., Fujiwara, N., Weibman, A. R., and Baker, H. (2016) Cytoarchitectural changes in the olfactory bulb of Parkinson's disease patients. *NPJ Parkinsons Dis.* **2**, 16011
51. Nakai, W., Kondo, Y., Saitoh, A., Naito, T., Nakayama, K., and Shin, H. W. (2013) ARF1 and ARF4 regulate recycling endosomal morphology and retrograde transport from endosomes to the Golgi apparatus. *Mol. Biol. Cell* **24**, 2570–2581
52. Kobayashi, N., Kon, S., Henmi, Y., Funaki, T., Satake, M., and Tanabe, K. (2014) The Arf GTPase-activating protein SMAP1 promotes transferrin receptor endocytosis and interacts with SMAP2. *Biochem. Biophys. Res. Commun.* **453**, 473–479
53. Fjorback, A. W., Müller, H. K., and Wiborg, O. (2009) Membrane glycoprotein M6B interacts with the human serotonin transporter. *J. Mol. Neurosci.* **37**, 191–200

Received for publication March 2, 2019.
Accepted for publication June 17, 2019.